Controlled star poly(2-oxazoline)s: Synthesis, characterization

Laetitia Plet, Gwendoline Delecourt, Mohamed Hanafi, Nadège Pantoustier, Gaelle Pembouong, Patrick Midoux, Véronique Bennevault, Philippe Guégan

Controlled star poly(2-oxazoline)s: Synthesis, characterization

Laetitia Plet[a], Gwendoline Delecourt[a], Mohamed Hanafi[b], Nadège Pantoustier[b], Gaëlle Pembouong[a], Patrick Midoux[c], Véronique Bennevault[a,d,*], Philippe Guégan[a,*]

[a] Institut Parisien de Chimie Moléculaire, UMR 8232 CNRS, Sorbonne Université, Paris, France
[b] Sciences et Ingénierie de la Matière Molle, ESPCI Paris, PSL University, CNRS, Sorbonne Université, Paris, France
[c] Centre Biophysique Moléculaire, UPR 4301 CNRS, Orléans, France
[d] University of Evry, Evry, France

ARTICLE INFO

Keywords:
2-oxazoline polymerization
Pluritriflate initiators
Star polymers

ABSTRACT

Poly(2-methyl-2-oxazoline) and poly(2-ethyl-2-oxazoline) star polymers with 3, 4 and 6 arms are synthesized from pluritriflate initiators. Characterization of the topology was achieved by NMR, SEC and kinetic studies. The initiation step of 2-ethyl-2-oxazoline being slow, heterogeneous star polymers in arm molar masses are obtained for low molar mass polymers. However, for both monomers, high molar mass homogeneous star polymers are obtained. A fast initiation is observed for the polymerization of 2-methyl-2-oxazoline, providing a control of the topology even at low molar mass. In the studied molar mass range, linear kinetic first order plots and linear molar mass as a function of conversion are obtained for both monomers, suggesting living polymerizations.

1. Introduction

Polymerization of oxazolines, especially the polymerization of oxazolines substituted in the 2-position, has been intensively studied for more than 50 years. Due to steric hindrance, the monomers substituted in 4 and 5 position are difficult to polymerize [1], while well-defined poly(2-oxazoline)s (POx) are synthesized by cationic ring-opening polymerization (CROP) of 2-oxazolines [2]. Usual initiators are strong protonic acids or their esters, Lewis acids, alkyl halides [2]. An ionic and a covalent mechanisms can coexist depending upon the relative nucleophilicity of the monomer and counter-anion [2] and the operating conditions [3–5]. The water-soluble properties of some POx such as poly(2-methyl-2-oxazoline)s (PMeOx) or poly(2-ethyl-2-oxazoline)s (PEtOx) make them ideal candidates for biological applications. The biocompatibility of POx has been demonstrated [6] and the pseudo-peptide concept was suggested to emphasize the close structural similarity between polyoxazolines and polypeptides [7].

Poly(ethylene oxide) (PEO) has been the gold standard in the biomedical field and more particularly in drug delivery thanks to its biocompatibility, stealth behavior and ability to prolonged blood circulation when used as a corona for particles [8]. Number of FDA-approved "PEGylated" pharmaceuticals are on the market to treat several diseases [9]. However, some drawbacks of PEO have recently been published, questioning a systematic use of PEO for biomedical issues [10]. In this context, poly(2-oxazoline)s are proposed as a promising alternative for PEO [10].

The versatile 2-alkyl-2-oxazoline polymerization chemistry allows the synthesis of complex architectures such as block copolymers [11–13], star-shaped [14–16] or hyperbranched [17–19] polymers. Star polymers are composed of at least three linear arms spreading from a low molecular weight central core. Homogeneous star polymers and heterogeneous star polymers can be distinguished according to whether the arms are of same length and chemical nature or not. Qiu and Bae reviewed the importance of polymer topology on the drug delivery applications [20]. To date, the most used polymeric systems for drug delivery are the "polymeric micelles", made of amphiphilic block copolymer in which the hydrophilic block is most often composed of PEO and the hydrophobic block can be of various nature, poly(D-L-lactide), poly(ε-caprolactone) for instance [21]. In this "core-shell" structure, the hydrophobic drug is conjugated to the hydrophobic block thereby forming the core of the micelle. It is protected by the water-soluble block which constitutes the shell thus allowing its solubilization and increasing its stability. The star polymer-based micelles are more stable than amphiphilic copolymers-based micelles thanks to the covalently branching points of which they are composed. Kovar et al. [22] highlighted the advantages of star structure thanks to the design of an antibody-targeted N-(2-hydroxypropyl)methacrylamide (HPMA) copolymer-bound doxorubicin conjugates with star structure. A significant higher antitumor effect was revealed compared to its linear counterpart, attributed to a higher cellular internalization rate and longer

blood-elimination profile. Furthermore, the multi-arm structure of star polymers leads to a lower flexibility resulting in a reduced ability of reptation through pores smaller than their hydrodynamic radius. Thus, star-shaped polymers exhibit a difficulty to pass through glomerular pores that decreases the renal clearance, thus increase the circulation time [23]. While POx was largely investigated as a PEO substitute in drug delivery applications [24], only few reports on star POx synthesis were reported, with a limited number of arms and incomplete characterizations [14,25,26].

Two main strategies, named “arm-first” and “core-first” methods, are usually used to synthesize star-shaped polymers [27]. In the “arm-first” method [28], linear arm precursors are polymerized in a first step and a multifunctional termination agent is then added. The advantage of this method is that arms are prepared by living polymerization and easily characterized, ensuring the homogeneity of the future star arms. However, star polymers with large molar mass or high number of arms are difficult to synthesize, due to steric hindrance provided by the first arms linked to the core [28]. Moreover, further purification steps to eliminate the excess of linear polymer is a requirement to obtain pure compounds [29]. The “core-first” method [26,30,31] involves the use of a multifunctional initiator from which the polymer chains propagate. The main difficulty of this method is that the arms cannot be characterized beforehand, so the final star characterization is complicated and may be done by indirect methods. To synthesize homogeneous star polymers with arms of similar molar masses, all the initiating functions of the multifunctional initiator must exhibit the same reactivity [32] and the initiation rate must be greater than the propagation rate.

Synthesis of 3 and 4 arms star polymers using 2-methyl-2-oxazoline as monomer has been reported [25]. Larger molar masses star polymers and comparing the polymerization of 2-methyl and 2-ethyl-2-oxazoline initiated with the same plurifunctional initiators has not been reported yet. Furthermore, no 6-arms star POx have ever been synthesized. In this study, we report the use of different pluritriflate initiators for the CROP of 2-methyl-2-oxazoline and 2-ethyl-2-oxazoline in order to synthesize star architectures with 3, 4 and 6 arms. Therefore, an in-depth study was conducted to determine the real number of arms obtained for the synthesized polymers and to highlight the control of the polymerization. Kinetic investigations of the polymerizations by ^{1}H NMR and size exclusion chromatography analysis of the collected polymers are presented, and the results concerning both monomers will be compared.

2. Materials and methods

2.1. Materials

Acetonitrile (ACN) (purchased from VWR), 2-methyl-2-oxazoline (MeOx), 2-ethyl-2-oxazoline (EtOx) (purchased from Sigma-Aldrich) were dried by refluxing over calcium hydride for 24 h at least, under vacuum, and cryodistilled prior use. Termination agents (aniline, purchased from Sigma-Aldrich and morpholine, purchased from ABCR) were stored on a 3 $\dot{A}$ sieve activated by heating at 150 °C for 5 h under vacuum prior use. Pentarythritol, di(trimethylolpropane), 1,1,1-tris (hydroxymethyl)ethane and trifluoromethanesulfonic anhydride were purchased from Sigma while dipentaerythritol was purchased from Acros Organics. Ethyl trifluoromethanesulfonate (purchased from Sigma-Aldrich) was opened and stored into a glove box.

2.2. Synthesis of pluritriflate initiators

1,1,1-tris(hydroxymethyl)ethane tristriflate (I_3) and pentaerythritol tetratriflate (I_4) were synthesized according to literature [33]. Furthermore, an additional tetrafunctional molecule, di(trimethylolpropane) tetratriflate (I_{e4}) and an hexafunctional molecule, dipentaerythritol hexatriflate (I_{e6}), were synthesized by adapting literature procedure [33] and were characterized by ^{1}H, ^{13}C, 2D NMR and high resolution electrospray ionization mass spectrometry (HRMS-ESI). Di (trimethylolpropane) tetratriflate (I_{e4}) and dipentaerythritol hexatriflate (I_{e6}) present an ether bond in their core and so “e” stand for “ether” in their respective abbreviation. The typical procedure for a triflatation is reported for the synthesis of dipentaerythritol hexatriflate: a stirred suspension of 626.6 mg dipentaerythritol (2.46 mmol) in 4.0 mL of ACN and 2.5 mL of anhydrous pyridine was cooled at 0 °C. 5 g of triflic anhydride (17.7 mmol, 1.2 eq per alcohol function) were added dropwise over 30 min still at 0 °C. The reaction proceeds under agitation at room temperature for an additional 3 h before adding 20 mL of a 1 M HCl solution. Cooling in an ice bath allowed the precipitation of the product. The orange solid was filtered and washed with distilled water. Then, a hot ACN/H_2O (1/1) mixture was added. A liquid / liquid extraction was performed and an orange oil was recovered. After evaporation of the solvents and drying under vacuum at 30 °C for 6 h, 756 mg of orange solid were obtained (29% yield). I_{e4} was obtained with 81% yield using a similar protocol, without doing the liquid/liquid extraction.

^{1}H NMR (400 MHz, acetone-d_6) : I_3 : δ (ppm) = 4.92 ppm (s, 6H, CH_2-OTf), 1.40 (s, 3H, CH-CH_3); I_4 : δ (ppm) = 5.17 ppm (s, 8H, CH_2-OTf); I_{e4} : δ (ppm) = 4.80 (s, 8H, CH_2-OTf), 3.67 (s, 4H, O-CH_2-C-), 1.70 (q, 4H, C-CH_2-CH$_3$), 1.03 (t, 6H, C-CH$_2$-CH_3); I_{e6} : δ (ppm) = 5.06 (s, 12H, CH_2-OTf), 4.00 (s, 4H, O-CH_2-C-). HRMS (ESI): I_3 : calcd for $C_8H_9F_9O_9S_3 + Na^+$: 538.9157, found: 538.9161; I_4 : calcd for $C_9H_8F_{12}O_{12}S_4 + Na^+$: 686.8599, found: 686.8606; I_{e4} : calcd for $C_{16}H_{22}F_{12}O_{13}S_4 + Na^+$: 800.9644, found: 800.9667; I_{e6} : calcd for $C_{16}H_{16}F_{18}O_{19}S_6 + Na^+$: 1068.8215, found: 1068.8257. The spectra of all the initiators are provided in supporting information.

2.3. Synthesis of poly(2-methyl-2-oxazoline) (PMeOx) and poly(2-ethyl-2-oxazoline) (PEtOx)

MeOx and EtOx polymerizations were carried out in dry ACN as solvent, at 80 °C, in a 100 mL round bottom flask that was previously flamed under vacuum, then filled under inert atmosphere. The typical procedure was as follows (Run 5*, Table 3): 159 mg of I_3 ($3.08.10^{-4}$ mol), were dried overnight through a vacuum line, then solubilized in 10.7 mL of ACN in a glove-box. This solution and 5.8 mL of EtOx ($5.75.10^{-2}$ mol, 187 eq) were successively introduced into the reactor in the glove-box. The reactor was then heated at 80 °C out of the glove-box during the requested time. At the end of the polymerization, the reactor was cooled back to room temperature and 10 equivalents of quencher per initiating function were added to the reactive medium. The quenched polymer was stirred at room temperature for 5 days. A sample was taken off to calculate the conversion from a ^{1}H NMR spectrum of the final reaction medium. After evaporating the solvent and drying the product at 50 °C under vacuum overnight, the crude product was purified by dialysis against water using a 1 kDa regenerated cellulose membrane (spectra/pore®). The external water was changed after 1 h, 2 h, 17 h for a total time of 24 h. The 2-methyl-2-oxazoline polymerizations were quenched by aniline, while the 2-ethyl-2-oxazoline polymerizations were quenched by morpholine. The samples were freeze-dried prior analysis. Variations to this protocol can be found in Tables 1 and 3.

The kinetic studies of the MeOx or EtOx polymerizations were carried as previously described, using a 100 mL round-bottom flask equipped with a septum. Periodically, aliquots of the reaction mixture were taken off with a syringe and the samples were quenched with an excess of termination agent (aniline or morpholine). The quenched aliquots were analyzed by ^{1}H NMR to determine the monomer conversion (excepted for the kinetic study of the EtOx polymerization initiated by I_3, I_{e4} and I_{e6} with a ratio $[EtOx]_0/[I]_0$ = 188 where the aliquots were analyzed before any quenching). The samples were finally dried and analyzed by SEC.

Table 1
Polymerization of MeOx initiated by I_1, I_3, I_{e4} and I_{e6}.

Run	Initiator	time (h)	p[1] (%)	$M_{n\ theo}$ [2] (kg.mol^{-1})	$M_{n\ NMR}$ (kg.mol^{-1})	$M_{n\ SEC\ DMF}$ [3] (kg.mol^{-1})	$Đ$[3]	$M_{n\ SEC\ H2O}$ [4] (kg.mol^{-1})	$Đ$[4]	dn/dc[4]
1#	I_1	27.7	97.0	15.5	22.5	14.2	1.57	14.3	1.20	0.168
2#	I_3	6.5	96.6	15.4	29.0	7.3	1.43	8.1	1.22	0.165
3#	I_{e4}	6	98.5	15.8	21.8	6.6	1.34	7.0	1.15	0.160
4#	I_{e6}	5.25	100	16.0	22.7	5.1	1.65	6.3	1.24	0.163

$[M]_0 = 3.5\ mol\ L^{-1}$ and $[M]_0/[I]_0 = 188$.

Polymer quenched with aniline at room temperature then dialyzed once against methanol (solvent changed after 1 h, 2 h and 16 h).

[1] Conversion calculated from the reaction medium analysis by ^{1}H NMR.

[2] $M_{n\ theo} = [M]_0/[I]_0 \times p \times M_{MeOx}$. $[M]_0$, $[I]_0$, p and M_{MeOx} correspond respectively to the initial monomer and initiator concentrations, conversion and molar mass of repeat unit.

[3] Determined by SEC in DMF after dialysis, RI detector, PMMA calibration.

[4] Determined by SEC in H_2O after dialysis, Triple (RI/LS/viscosimetric) detector, M_n^{LS}.

2.4. Analytical techniques

NMR experiments: Spectra were recorded with a Bruker 300 or 400 MHz spectrometers in 5-mm diameter tubes, using deuterated chloroform or methanol at 300 K. The Diffusion-Ordered SpectroscopY (DOSY) experiments were carried out at 298 K using the ledbpgp2s.mod pulse sequence with a linear gradient of 16 steps between 5% and 95%. The maximum field gradient strength was equal to 5.54 G mm^{-1}. Before each diffusion experiment, the length of the gradient δ and the diffusion time Δ were optimized. The software used for data analysis was Topspin. The performed mathematical treatment of the data was described in a previous paper [34].

ESI-MS experiments: ESI-MS experiments were carried out using a LTQ-Orbitrap XL from Thermo Scientific (Thermo Fisher Scientific, Courtaboeuf, France) and operated in negative ionization mode, with a spray voltage at 3.2 kV. Applied voltages were 20 and 70 V for the ion transfer capillary and the tube lens, respectively. The ion transfer capillary was held at 275 °C. Detection was achieved in the Orbitrap with a resolution set to 100,000 (at *m/z* 400) and a *m/z* range between 200 and 4000 in profile mode. Spectrum was analyzed using the acquisition software XCalibur 2.1 (Thermo Fisher Scientific, Courtaboeuf, France). The automatic gain control (AGC) allowed accumulation of up to 2.10^5 ions for FTMS scans, Maximum injection time was set to 300 ms and 1 μscan was acquired. 10 μL was injected using a Thermo Finnigan Surveyor HPLC system (Thermo Fisher Scientific, Courtaboeuf, France) with a continuous infusion of methanol at 100 μL min^{-1}.

Size exclusion chromatography (SEC) in DMF: The number-average molar mass (M_n), the weight-average molar mass (M_w) and the dispersity ($Đ = M_w/M_n$) were determined by size exclusion chromatography (SEC) in N,N-dimethylformamide (DMF) (1 g L^{-1} LiBr) at 60 °C with a flow rate of 0.8 mL min^{-1}, using two PSS GRAM 1000 Å columns (8 × 300 mm; separation limits: 1 to 1000 kg mol^{-1}) and one PSS GRAM 30 Å (8 × 300 mm; separation limits: 0.1 to 10 kg mol^{-1}) coupled to a differential refractive index (RI) detector and a UV detector after calibration with poly(methyl methacrylate) (PMMA) standards. 0.1 mL of a 5 mg mL^{-1} polymer solutions is injected after filtration through a 0.22 μm pore size filter.

Size exclusion chromatography (SEC) in water: The number (M_n) and weight (M_w) average molar masses, as well as the dispersity ($Đ$), of the synthesized polymers were determined by size exclusion chromatography (SEC) in a 0.2 M $NaNO_3$ aqueous solution at 35 °C with a flow rate of 0.7 mL min^{-1} using a Viscotek SEC system (Viscotek VE 2001 GPC Solvent - GPC MAX - Sample Module and TDA 302 triple detector array) equipped with two SHODEX OH pack columns SB-806M HQ (13 μm, 300 mm × 8 mm). The polymers were injected at a concentration of 4 mg mL^{-1} after filtration through a 0.2 μm pore size membrane. The absolute molar masses were determined by the three in-line detectors (refractometer, viscometer, and light scattering) relying upon a calibration based on poly(ethylene oxide) or pullulan standards.

3. Results and discussion

3.1. Synthesis of pluritriflate initiators

Since the first description of CROP of 2-oxazolines 50 years ago, many initiators have been used including *p*-toluenesulfonates (tosylates) [35,36], trifluoromethanesulfonates (triflates) [37], *p*-nitrobenzenesulfonates (nosylates) [38,39]. In order to obtain a homogeneous family of initiators bearing 3, 4 and 6 initiating sites, families of esters (tosylates, nosylates and triflates) were synthesized starting from multifunctional alcohols. Nosylate initiators were obtained with yields that were too low to be further considered for this study. Pluritosylate initiators were also successfully synthesized, but did not lead to any polymerization in the tested conditions (conventional heating at 80 °C). The pluritriflate initiators family was finally chosen as 2-alkyl-2-oxazoline polymerization initiators because of their convenient synthesis and purification combined to the high reactivity of the triflate function. Indeed, according to previous work, the use of pluritriflate initiators for the CROP of 2-oxazoline leads to fast quantitative initiation, [25] compared to plurihalides or pluritosylates initators [31].

1,1,1-tris(hydroxymethyl)ethane tristriflate (I_3), pentaerythritol tetratriflate (I_4), di(trimethylolpropane) tetratriflate (I_{e4}) and dipentaerythritol hexatriflate (I_{e6}) were successfully synthesized providing respectively tri, tetra and hexafunctional initiators (Fig. 1). The plurifunctional oxazoline polymerization initiators containing an ether function are investigated for the first time. Complete characterizations of the initiators are reported in SI (Figs. S1 to S12). The attributions of the peaks were confirmed thanks to 2D NMR. Quantitative reactions were confirmed by the total absence of signals belonging to the methylene groups CH_2-OH in ^{1}H NMR and in ^{13}C NMR, and the presence of the expected peaks in HRMS-ESI.

3.2. Synthesis of poly(2-methyl-2-oxazoline)s (PMeOx) star polymers

3.2.1. Synthesis

The three initiators (I_3, I_{e4} and I_6) described in Fig. 1 were used in order to synthesize 3-arms, 4-arms and 6-arms star poly(2-methyl-2-oxazoline)s (PMeOx) respectively. A linear PMeOx was also synthesized as a reference, using commercial ethyl triflate (I_1) as initiator. All the polymerizations were performed at a constant monomer concentration of 3.5 mol L^{-1} and the quenching was ensured by addition of 10 eq of aniline. Targeting a molar mass of 16 kg mol^{-1}, the monomer to initiator ratio was fixed at 188. The polymerizations were stopped when nearly total conversion was reached. The conversion *p* was evaluated from the ^{1}H NMR spectrum of the reaction medium using the peaks of the methylene protons of remaining monomer at $\delta = 4.12$ and 3.69 ppm and the peak of the methylene polymer backbone protons at $\delta = 3.37$ ppm. The characteristics of the obtained polymers are listed in Table 1.

SEC analyses were performed using two different lines in order to

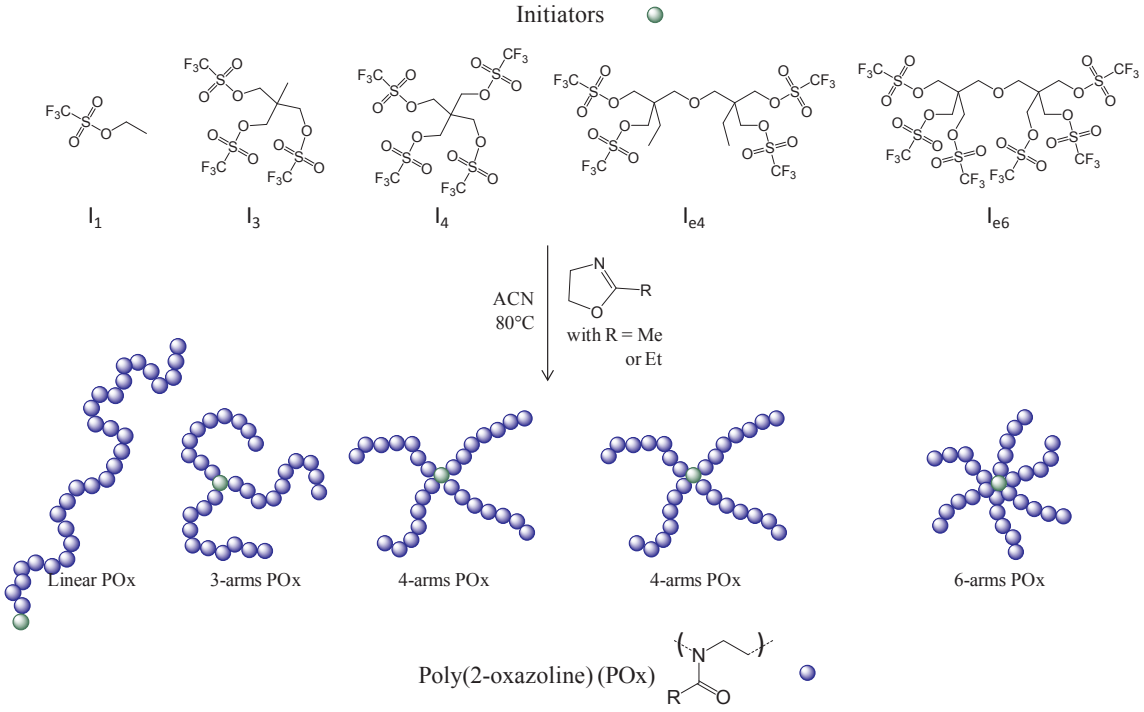

Fig. 1. Structures of the 5 initiators used to synthesize linear, 3-arms, 4-arms and 6-arms POx.

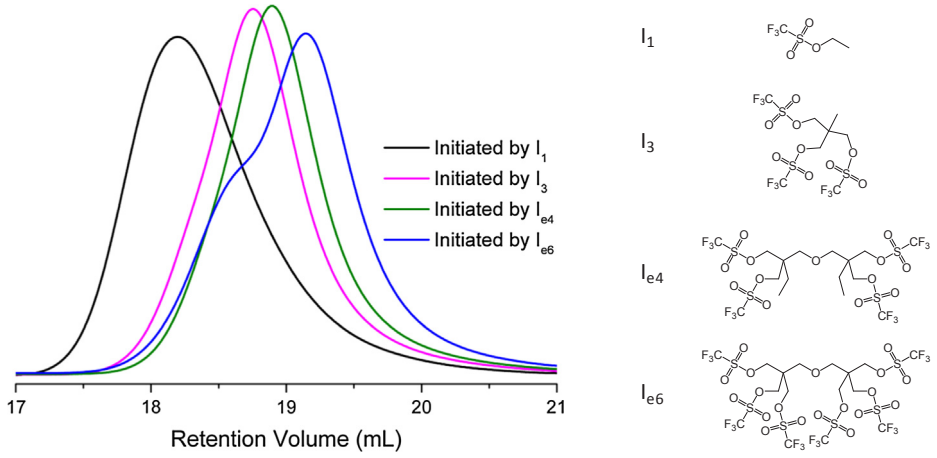

Fig. 2. SEC traces (H_2O, RI detection) of the PMeOx synthesized from mono (I_1), tri (I_3), tetra (I_{e4}) and hexa- (I_{e6}) functional initiator.

confirm the expected star topology. To show the compactness of the star structure, the apparent molar masses of all stars were calculated using the calibration made with linear PMMA standards calibration using a RI detector in SEC DMF. The apparent molar mass of the linear PMeOx ($14.2\,kg\,mol^{-1}$) is in good agreement with the theoretical value ($M_{n\ theo} = 15.5\,kg\,mol^{-1}$). As expected, the apparent molar masses of the star polymers are lower than the $M_{n\ theo}$. This is easily explained by the compact structure of the star polymers, which induces a lower hydrodynamic volume when compared to their linear counterpart. Furthermore, the hydrodynamic volume of star polymers decreases with the arm number increase, for a constant molar mass. Indeed, the hydrodynamic volume of the star PMeOx synthesized with I_{e6} is lower than the one of the star PMeOx synthesized with I_{e4}, respectively lower than one of the star PMeOx synthesized with I_3. The molar masses of these star polymers were also measured using SEC with triple detection (differential refractive index (RI) – light scattering (LS) and viscosimetric detectors) in water. Unexpectedly, SEC-analysis gives low nominal values when compared to the theoretical molar masses. Nevertheless, PMeOx initiated by I_1, I_3, I_{e4} and I_{e6} reveal narrow molar mass distributions (Fig. 2) with fairly good dispersity ($Đ$) around 1.20 and monomodal molar mass distribution with symmetric peak shapes (except for run $4^{\#}$, initiated with I_{e6}). The shoulder observed for the 6-arms star PMeOx, whose ratio varies according to the solvent used for the SEC analysis (Fig. S13), was assigned to polymer aggregation as already demonstrated for other systems [40]. To confirm this interpretation, a DOSY NMR experiment of this polymer was conducted in CD_3OD, which has a high affinity for PMeOx. The pseudo 2D spectrum obtained is presented in Fig. S14a. From the different proton peaks, a diffusion coefficient equal to $(1.54 \pm 0.04)\cdot10^{-10}\,m^2\,s^{-1}$ was determined. The low value of the standard deviation obtained suggests a well-defined structure of the star polymer. Moreover, for all the diffusants investigated in this study, monoexponential decays were observed, indicating that the self-diffusion coefficients are monodisperse, thus that the sample was homogeneous. The logarithm of the intensity of the methyl protons at 2.1 ppm versus $\gamma^2g^2\delta^2(\Delta - \delta/3)$ plot is given for example in Fig. S14b. This analysis shows also that the aniline used

to deactivate the active centers at the end of the polymerization is covalently linked to the polymer, since the aniline protons diffuse with the same diffusion coefficient as the polymer backbone protons.

The polymers obtained after dialysis were characterized by ^{1}H NMR. An example of ^{1}H NMR spectrum of run 3$^{\#}$ (Table 1) is given in supporting information (Fig. S15). The backbone proton of methylene and methyl group appeared respectively at 3.46 ppm and 2.10 ppm. NMR signals of protons of the star core are not identified: signals of CH_2-O are probably hidden under the signal of the polymer unit CH_2-N at 3.46 ppm and the rigidity of the polymer core leads to signals spreading, making it impossible to detect. The aniline end-functions were used to calculate the molar mass of the polymers ($M_{n\ NMR}$), but this calculation leads to a value 1.5 higher than $M_{n\ theo}$ explained by a partial functionalization by aniline for the star polymers. A similar trend is observed for the linear one (run 1$^{\#}$, Table 1, $M_{n\ NMR} = 22.5\ kg\ mol^{-1}$).

3.2.2. Branching study of PMeOx star polymers

When compared to a linear polymer of same molar mass, a branched polymer exhibits a lower hydrodynamic volume and as a consequence, a lower intrinsic viscosity since the hydrodynamic volume is correlated to the molar mass (MM) multiplied by the intrinsic viscosity. The Zimm and Stockmayer theory [41] defines the geometric branching factor, g, as the ratio of the square of the gyration radius of the branched polymer ($R_{g\ branched}$) to the linear polymer one ($R_{g\ linear}$), for a same molar mass (Eq. (1)). Their random walk theory predicts that:

$$g = \left(\frac{R^2_{g,branched}}{R^2_{g,linear}} \right)_{MM} \quad (1)$$

The radius of gyration R_g is measured by light scattering, however, this measure is not possible when R_g is lower than 15 nm. In this case, the branching ratio g' defined by Zimm et Kilb [42] as the ratio of the intrinsic viscosities of branched ($[\eta]_{branched}$) to the linear polymer one ($[\eta]_{linear}$) with the same molar mass can describe the contraction phenomena (Eq. (2)):

$$g' = \left(\frac{[\eta]_{branched}}{[\eta]_{linear}} \right)_{MM} \quad (2)$$

The branching ratio g′ from Eq. (2) calculated for polymer stars decreases with increasing number of arms. It has been experimentally proven that g and g' are correlated according to the following equation:

$$g' = g^{\varepsilon} \quad \text{with} \quad 0.5 \leq \varepsilon \leq 1.5 \quad (3)$$

The intrinsic viscosities of the different star polymers were then measured thanks to a viscosimetric detector coupled to the water-SEC line allowing the calculation of the branching ratio g'. Thanks to the viscosimetric detector, the intrinsic viscosity of each polymer was obtained across the molar mass distribution. As expected according to the equation of Mark-Houwink ($[\eta] = KM^{\alpha}$), the log–log plots are linear and the intrinsic viscosities of stars are lower than the intrinsic viscosity of the linear polymer, and the more arms the star contains, the lower the intrinsic viscosity is (Fig. 3). In the Mark-Houwink equation, the exponent α is relative to the contraction of the polymer in solution. Again, the star polymer contraction in solution increases with the number of arms, for a constant molar mass [43]. In our study, α = 0.75 for I_1, α = 0.71 for I_3, α = 0.65 for I_{e4} and α = 0.56 for I_{e6}, following the expected trend. The observed linearity of the log–log plot of intrinsic viscosity versus molar mass is consistent with a constant amount of branching for all stars all over the molar mass distribution (Fig. 3).

To go further, the arm number f can be calculated by setting an appropriate value of ε and calculating the geometric branching factor g. The ε values range from 0.5 to 1.5 depending on the architecture of the polymer. For a star polymer, the theoretical value is $\varepsilon = 0.5$ in a theta solvent; however it was empirically shown that this value can vary. In this study, the arm numbers f initially calculated by imposing $\varepsilon = 0.5$ were significantly higher than the expected ones ($f = 3.7$ for PMeOx initiated by I_3; $f = 4.9$ for PMeOx initiated by I_{e4} and $f = 9.4$ for PMeOx initiated by I_{e6}). The assumption of coupling reactions was not considered since the polymers SEC traces of the polymers initiated by I_3 and I_{e4} were monomodal. The α values obtained from Fig. 3 demonstrate that water is not a theta solvent in our conditions, questioning the choice of $\varepsilon = 0.5$. Furthermore, Jackson et al. [44] found that $\varepsilon = 0.79$ was the most appropriate value for polystyrene stars in THF. As highlighted by Balke et al. [45], this uncertainty about ε generates a substantial uncertainty about the arm number f. Therefore, in order to determine consistent values of ε for each star PMeOx, regardless of the structure of the star, another approach was taken, based on Jackson's approach [44].

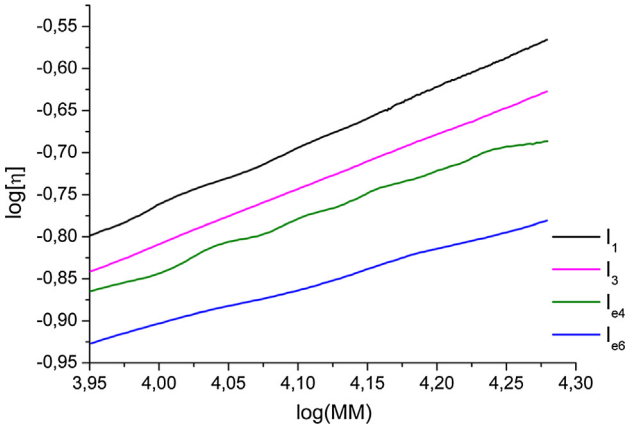

Fig. 3. Log-log plot of intrinsic viscosity as a function of molar masses of PMeOx synthesized from mono (I_1), tri (I_3), tetra (I_{e4}) and hexa- (I_{e6}) functional initiator (Mark-Houwink plot).

The level of functionality of star polymers can be modeled using the relationship, which exists between g and number of arms (functionality). The g_{theo} was calculated from Eqs. (4) or (5) using the theoretical arm number f

$$g = \frac{3f - 2}{f^2} \quad \text{for monodisperse arms stars} \quad (4)$$

$$g = \frac{3f}{(f+1)^2} \quad \text{for polydisperse arms stars} \quad (5)$$

f representing the arm number of the star polymer.

From this g_{theo} and the g'_{exp} obtained by viscosimetry measurements, a "semi-experimental ε" was determined. The ε values obtained starting from Eq. (4) with the hypothesis of stars with monodisperse arms are higher than the theoretical range (0.5 to 1.5) and vary a lot so the hypothesis of stars with polydisperse arms was considered as the most suitable in our case. These ε values (0.84 for PMeOx initiated by I_3; 0.85 for PMeOx initiated by I_{e4} and 0.74 for PMeOx initiated by I_{e6}) were introduced in the SEC-software and led to the arm number values (f_{exp}) considering the overall distribution of the polymers (Table 2). These ε are very close to the one determined by Jackson et al. [44] for solutions of PS in THF, and this strengthens our initial assumption. Secondly, the semi-experimental arm number values that are determined are close to the expected ones, independently of the arm number. The f value is even slightly higher than the expected one for the *hexa*-arms star polymers, which is in favor of the participation of each initiating sites of I_{e6} to the formation of the star polymers.

3.2.3. Kinetic study of MeOx polymerization using tristriflate (I_3), di (trimethylolpropane) tetratriflate (I_{e4}) and hexatriflate (I_{e6}) intiators

The demonstration by physico-chemical analyses that the number of arms of star polymers correspond exactly to the expected one remains a challenge, and Luxenhofer et al. [25] suggested using kinetic analyses

Table 2
Calculations of ε and f_{exp}.

f_{theo}	g'_{exp}	g_{theo} considering monodisperse arms star[1]	g_{theo} considering polydisperse arms star[2]	ε considering monodisperse arms star	ε considering polydisperse arms star	f_{exp} considering polydisperse arms star
3	0.616	0.778	0.562	1.93	0.84	2.9
4	0.536	0.625	0.480	1.33	0.85	3.7
6	0.476	0.444	0.367	0.91	0.74	6.6

[1] Calculated with Eq. (4).
[2] Calculated with Eq. (5).

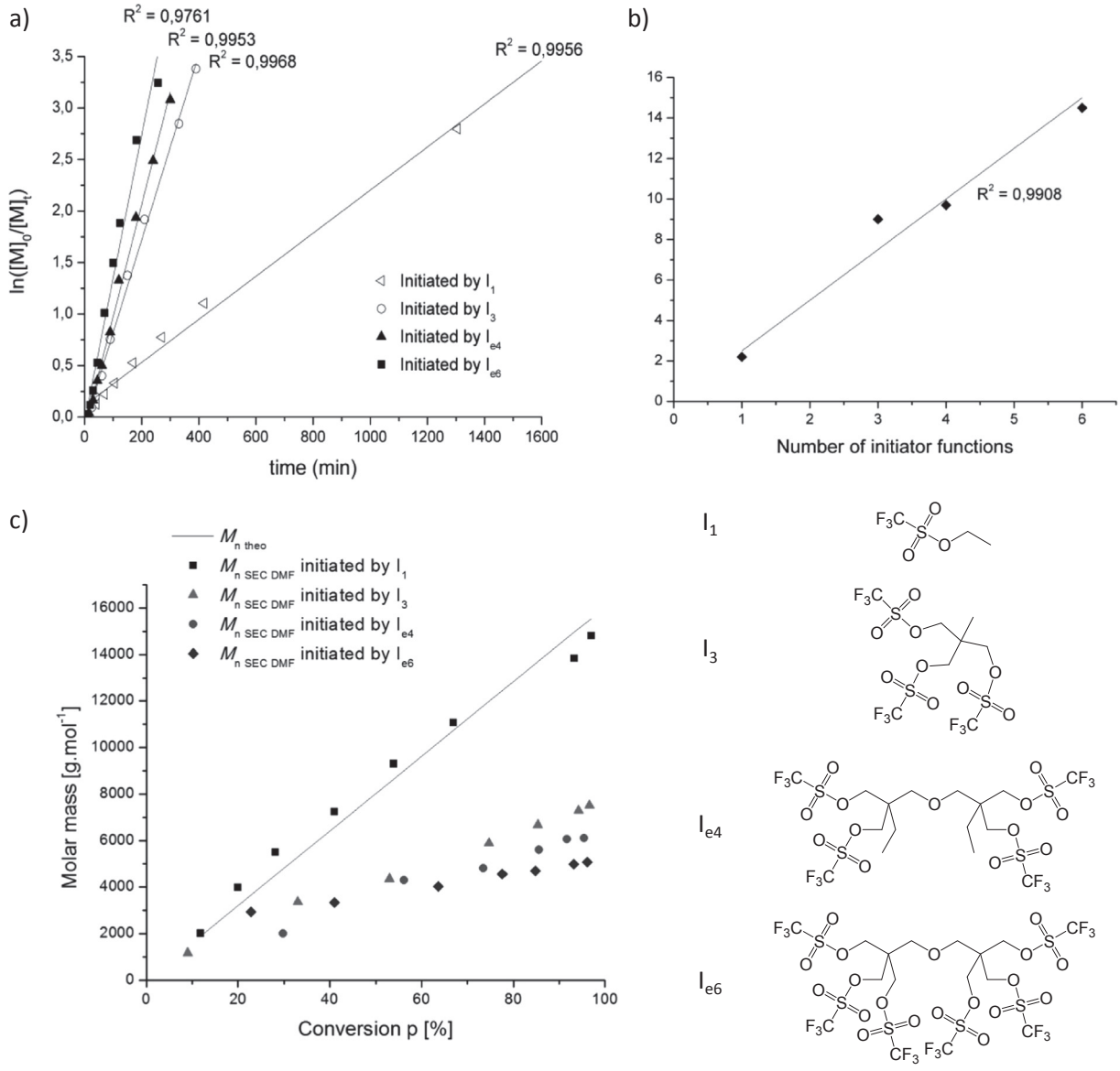

Fig. 4. Polymerization of MeOx using initiators I_1, I_3, I_{e4} and I_{e6} with $[MeOx]_0/[I]_0 = 188$: (a) linear first order kinetic plots; (b) relation between the number of triflate initiating groups per initiator and the propagation rate constant k_p^{app}; (c) molar masses of linear and star PMeOx as a function of conversion.

to support the physico-chemical analysis. MeOx polymerization using bis-, tris- and tetra-kistriflate initiators for a monomer to initiator ratio of 80 with a MeOx concentration of 0.7 mol L^{-1} were conducted, and occurred without any significant termination or transfer reactions. The k_p^{app} measured with the different plurifunctional initiators were plotted as a function of the arm number of the investigated initiator. The increase of the k_p^{app} as a function of arm number was demonstrated, with a nearly discrete increase of k_p^{app} as a function of arms number, for the two multifunctional initiators used in their study [25]. We thus conducted similar experiments in order to complete these results and investigate the polymerization of MeOx using a new tetratriflate initiator (I_{e4}) and a more sterically hindered hexatriflate initiator (I_{e6}). For each polymerization, samples were taken off periodically for ^1H NMR analysis and the conversion was determined as previously described, *i.e.* after mixing the sample with an excess of aniline for 3 min to deactivate the active centers. The four pseudo-first order plots of ln $([M]_0/[M]_t)$ versus time reveal a linear relationship ($R^2 > 0.976$) indicating a constant number of propagating centers during the overall

polymerization time (Fig. 4a). This result suggests that the polymerization proceeds with a fast initiation step so that all the arms of the polymer chains start growing simultaneously. As a consequence, the polymerization rate is defined by the propagation step. The k_p^{app} is calculated using the equation below:

$$\ln\left(\frac{[M]_0}{[M]_t}\right) = k_p^{app} \times [I]_0 \times t \quad (6)$$

with $[I]_0$ corresponding to the initial concentration of initiator, $[M]_0$ the initial monomer concentration and $[M]_t$ the monomer concentration at time t.

k_p^{app} extracted from the pseudo-first order plots increase with the functionality of the used initiator. Then, the propagation rate constants k_p^{app} were plotted against the number of initiating functions carried by the used initiator (Fig. 4b). The linearity of the plot indicates that all the triflate groups of I_3, I_{e4} and I_{e6} are of equal reactivity leading to a quantitative initiation and so to well-defined star PMeOx. Furthermore, all the samples of these polymerizations were dried and analyzed by DMF SEC. The linear increase of M_n versus conversion observed for the four polymerizations (Fig. 4c) shows that no significant transfer reaction occurred during the polymerization time. The superposition of the samples chromatograms obtained by SEC in DMF is provided for run 3# (Table 1) in Fig. S16. All the measured M_n for star polymers are lower than the theoretical one as expected, considering that the M_n were determined using a calibration with PMMA standards. However, a good agreement between theoretical and measured molar mass is obtained for the linear polymer. All together, these results suggest a living polymerization of MeOx in these conditions.

3.3. Synthesis of poly(2-ethyl-2-oxazoline)s (PEtOx) star polymers

3.3.1. Synthesis

2-ethyl-2-oxazoline polymerization is well-known to proceed in a more controlled manner, allowing the synthesis of controlled PEtOx with high molar mass [36,46]. In the present work, EtOx was polymerized using the initiators previously described at different monomer to initiator ratios to target three number average degrees of polymerization, $X_{n\ targeted}$, respectively 590, 370 and 188 in order to compare these polymerizations to the previous PMeOx syntheses. The initial monomer concentration $[M]_0$ is set to 3.5 mol L^{-1}. The termination step for the EtOx polymerizations was carried out by addition of 10 eq of morpholine, expecting a more efficient quenching of the growing species. The morpholine functions were subsequently used to calculate the molar mass of the polymers by NMR ($M_{n\ NMR}$), except for the higher molar mass polymers due to the increased uncertainty. All obtained data are gathered in Table 3. Nearly complete conversions are obtained, as for MeOx. Conversion is determined from the ^{1}H NMR spectra of the reaction media using the peaks of the initial monomer at δ = 4.16 and 3.73 ppm and the peak of the resulting polymer at δ = 3.34 ppm. On the ^{1}H NMR spectrum of run 5* (Fig. 5), the peak corresponding to the methylene protons of the polymer backbone at δ = 3.33 ppm, the peaks corresponding to the methylene and methyl protons of the pendant groups, respectively at δ = 2.28–2.19 ppm and δ = 0.99 ppm, and the peaks corresponding to methylene protons adjacent to the amine or ether function of the morpholine end chains at δ = 2.35 ppm and 3.55 ppm are evidenced. The attribution was confirmed thanks to COSY and DOSY NMR experiments (Figs. S17 and S18). Indeed, the DOSY NMR spectrum shows that the peaks at 2.35 ppm and 3.55 ppm belong to morpholine covalently linked to the polymer chains, since they present the same diffusion coefficient as the polymer protons. Residual free morpholine was also observed at 2.97 ppm and 3.70 ppm. Considering all the polymer NMR peaks, a diffusion coefficient equal to $(1.68 \pm 0.09)\cdot10^{-10}$ $m^2\,s^{-1}$ was determined. The low value of the standard deviation and the observation of monoexponential decays for all the diffusants suggest a well-defined structure of the star polymer.

Concerning the lowest molar mass polymers initiated by I_3 and I_4 (respectively run 5* and run 8*), a relatively good agreement between $M_{n\ theo}$ and $M_{n\ NMR}$ is obtained. The latter was determined from the peak intensity ratio of the methylene protons of the polymer backbone (3.33 ppm) and the methylene proton of the morpholine group (3.55 ppm) located at the end of the macromolecular chain. These results suggest that the deactivation reaction of the growing species by morpholine is quantitative. The $M_{n\ NMR}$ of star polymers with larger molar masses could not be determined through this method due to NMR accuracy.

For all the characterized star polymers presented in Table 3, a narrower distribution is obtained when the star polymers are analyzed in SEC in water. SEC chromatograms of the star PEtOx obtained with the different pluritriflate initiators are presented Fig. 6. In each series ($[EtOx]_0/[I]_0$ = 188, $[EtOx]_0/[I]_0$ = 370, $[EtOx]_0/[I]_0$ = 590), a shift of the signal toward high elution volume is observed with increasing arm number of the star. All the star polymers present narrow and monomodal molar mass distributions with $Đ < 1.22$, even the PEtOx initiated by I_{e6} with $[EtOx]_0/[I]_0$ = 590 which presents a very slight shoulder. This last polymer was also characterized by DOSY NMR in CD_3OD to discriminate a side reaction from a star polymer aggregation during the analysis (Fig. S19). The mathematical treatment of all the polymer NMR signals conducted to an average diffusion coefficient equal to $(9.5 \pm 0.2)\cdot10^{-11}$ $m^2\,s^{-1}$. In addition to the low standard deviation of the diffusion coefficient, a linear ln I versus $\gamma^2g^2\delta^2(\Delta - \delta/$

Table 3
EtOx polymerizations initiated by I_3, I_4, I_{e4} or I_{e6}.

Run	Initiator	$[M]_0/[I]_0$	t (h)	p[1] (%)	$M_{n\ theo}$ [2] (kg mol^{-1})	$M_{n\ NMR}$ [3] (kg mol^{-1})	$M_{n\ SEC\ DMF}$ [4] (kg mol^{-1})	$Đ$ [4]	$M_{n\ SEC\ H2O}$ [5] (kg mol^{-1})	$Đ$ [5]	dn/dc [5]
5*	I_3	188.0	15	100	18.6	18.0	7.6	1.31	7.4	1.09	0.150
6*	I_3	370.5	24	100	36.7	–	12.9	1.27	12.2	1.06	0.170
7#	I_3	585.0	28	99	57.4	–	17.0	1.53	17.6	1.15	0.164
8*	I_4	188.0	15	100	18.6	13.0	6.8	1.39	6.9	1.14	0.164
9*	I_{e4}	187.7	5.2	97	18.0		7.1	1.40			
10*	I_4	374.4	24	100	37.1	–	11.5	1.33	10.6	1.10	0.177
11*	I_4	591.0	42	100	58.6	–	17.7	1.39	16.9	1.11	0.169
12#	I_{e4}	589.3	28	97	56.5	–	16.2	1.64	16.3	1.21	0.165
13#	I_{e6}	588.4	28	100	58.0	–	12.8	1.52	12.4	1.22	0.163

$[M]_0$ = 3.5 mol L^{-1}.

Polymer quenched by aniline at room temperature for 4 days and dialyzed once in MeOH (1 h + 1 h + 16 h).

* Polymer quenched by morpholine at room temperature for 5 days and dialyzed once in H_2O (1 h + 2 h + 16 h + 5 h).

[1] Conversion calculated from the reaction medium analysis by ^{1}H NMR.

[2] $M_{n\ theo} = [M]_0/[I]_0 \times p \times M_0$.

[3] Determined by ^{1}H NMR after dialysis.

[4] Determined by SEC in DMF after dialysis, RI detector, PMMA calibration.

[5] Determined by SEC in H_2O after dialysis, Triple (RI/LS/viscosimetric) detector, M_n^{LS}.

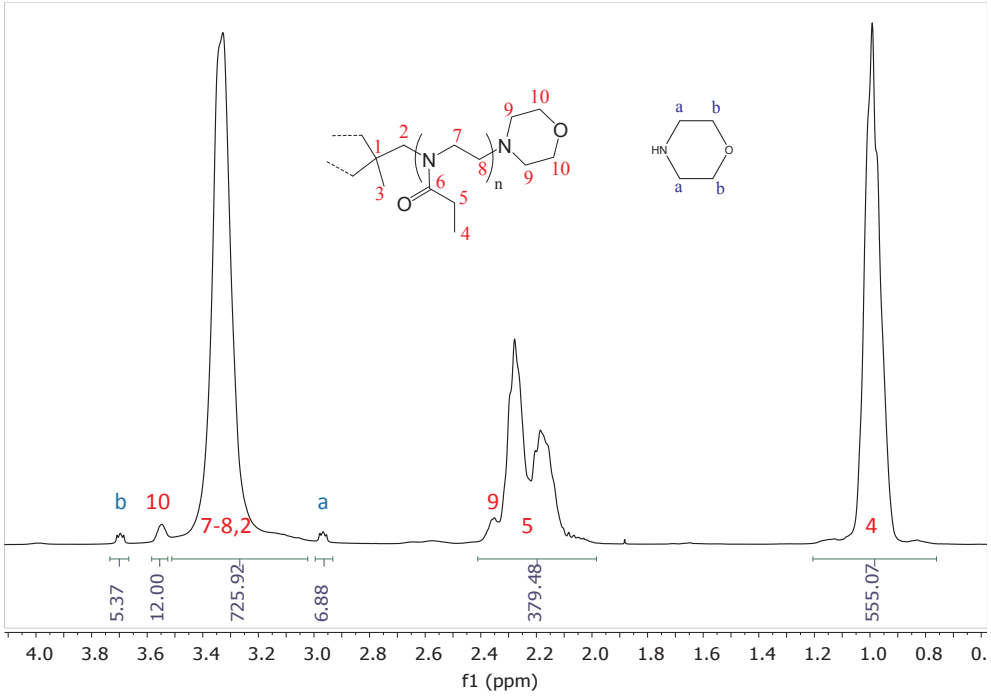

Fig. 5. ^{1}H NMR of 3-arms star (run 5*, Table 3) in $CDCl_3$.

3) plot was observed for each signal, indicating a well-defined structure of the star polymer. The comparison of the analyses of runs 11* and 12# shows that the presence of ether bond in the tetrafunctional initiator does not have any influence on the 2-ethyl-2-oxazoline polymerization, as expected.

The NMR and SEC characterizations of star poly(2-ethyl-2-oxazoline)s suggest that the synthesis of controlled star polymers is achieved. With this study, we believe that all the polymers have a same molar mass, thus similar structure. However, the heterogeneity of the arms molar mass could be discussed, and this point alleviate by a kinetic analysis.

3.3.2. *Kinetics of polymerization of EtOx using tristriflate (I_3), tetratriflate (I_4 and I_{e4}) and hexatriflate (I_{e6}) intiators*

Kinetic studies of polymerization of EtOx were performed using a $[EtOx]_0/[I]_0$ ratio equal to 590 or 188, following the conditions presented in Table 3. First, the $[EtOx]_0/[I]_0$ ratio is set to 590. The plots of $\ln([M]_0/[M]_t)$ versus time are presented Fig. 7a for the four initiators, and the expected linear relationship is obtained ($R^2 > 0.994$), indicating a constant number of propagating centers. The propagations rate constants k_p^{app} are plotted against the number of initiating functions borne by the used initiator (Fig. 7c). As for MeOx polymerization, a linear increase of the k_p^{app} versus the number of initiating sites is observed. An equal reactivity of all the triflate groups whatever the initiator is thus demonstrated, and an apparent fast initiation is shown in these polymerization conditions. The k_p^{app} values for EtOx polymerization are very closed to the ones of MeOx polymerization. (Table S1). The k_p^{app} value of $2.2.10^{-3}\,L\,mol^{-1}\,s^{-1}$ obtained for the initiation with I_1 (EtOTf) is the same order than the one reported by Hoogenboom et al. [37]. The polymerization kinetic of 2-methyl-2-oxazoline is usually higher than the one of 2-ethyl-2-oxazoline, as mentioned by Hoogenboom et al. [37] working at 80 °C in DMAc : $(2.51 \pm 3.9)\cdot10^{-3}\,L\,mol^{-1}\,s^{-1}$ for MeOx and $(1.62 \pm 4.2)\cdot10^{-3}\,L\,mol^{-1}\,s^{-1}$ for EtOx. However, we find out that the polymerization kinetics in the present study converge toward the same value in acetonitrile at 80 °C using a conventional heating. A more recent study using microwaves heating conditions was reported by Hoogenboom and coll. [39]. They reported a propagation kinetic constant of $4.35.10^{-3}\,L\,mol^{-1}\,s^{-1}$ for a polymerization conducted at 80 °C with a EtOx concentration of 4 mol L^{-1} for initiator to monomer ratio of 1:50. A slight difference is noticed with our results probably because of the reaction conditions. The convergence of polymerization kinetics of 2-methyl-2-oxazoline

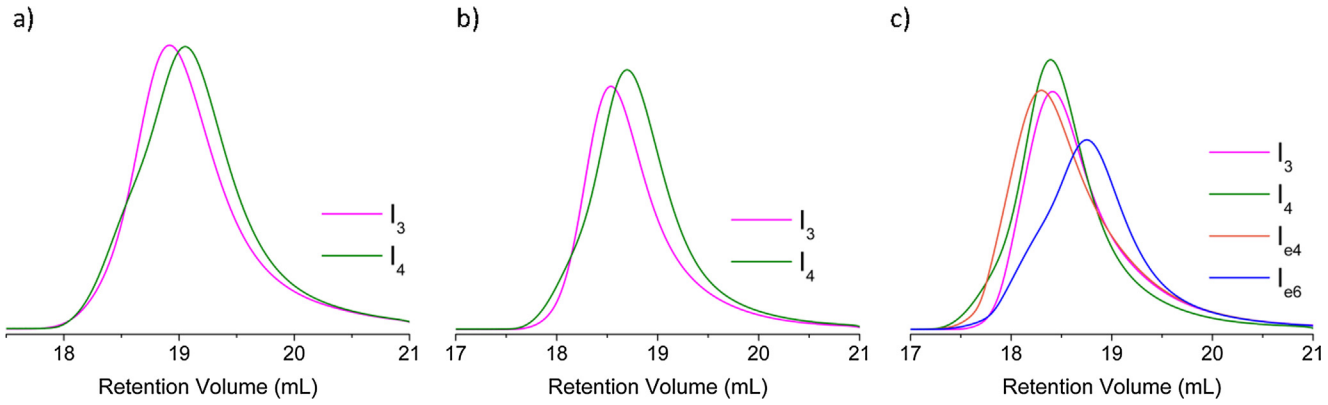

Fig. 6. SEC traces (H_2O, RI detection) of the PEtOx synthesized with (a) $[EtOx]_0/[I]_0 = 188$; (b) $[EtOx]_0/[I]_0 = 370$; (c) $[EtOx]_0/[I]_0 = 590$.

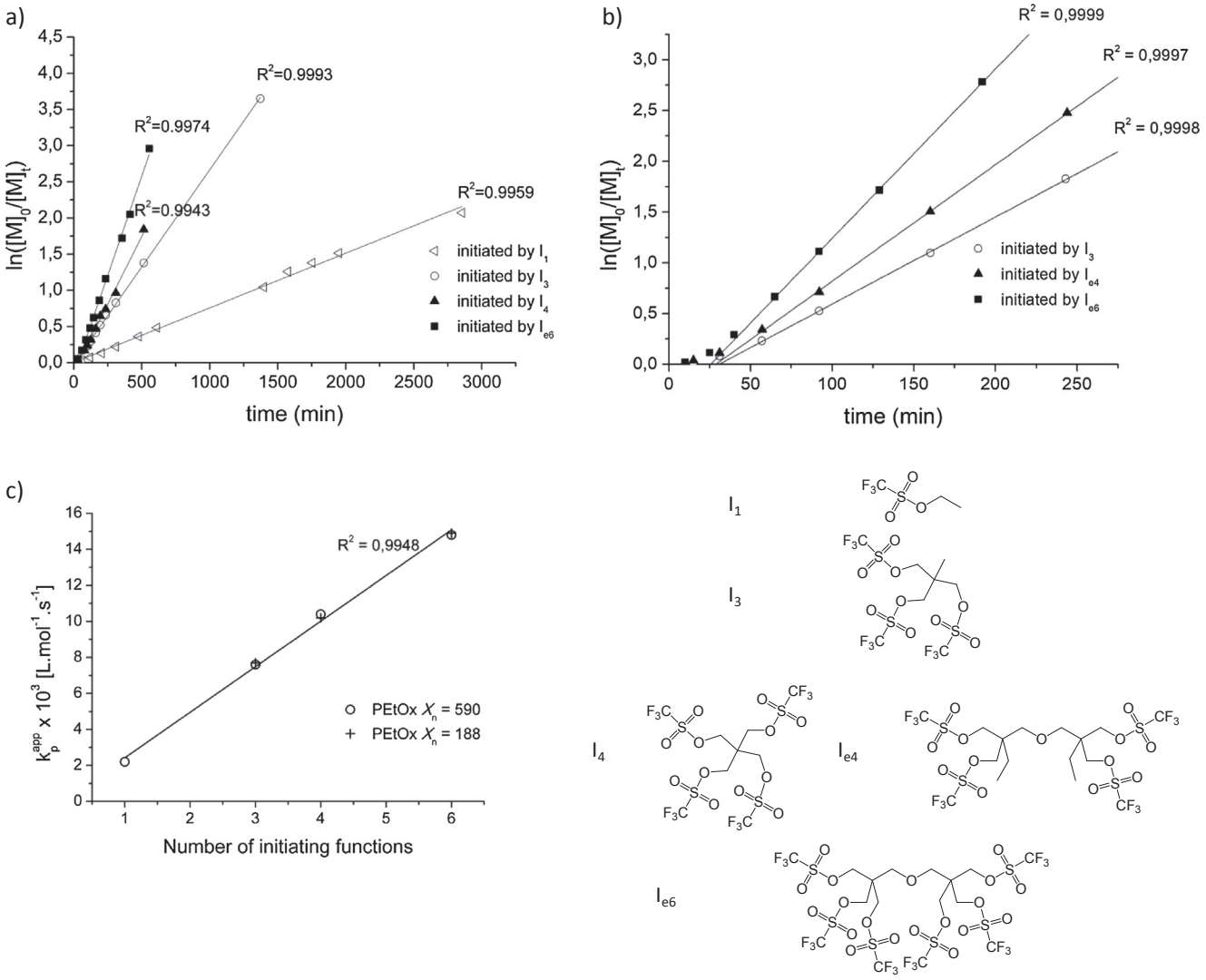

Fig. 7. Polymerization of EtOx: (a) linear first order kinetic plots for the polymerizations using initiators I_1, I_3, I_4 and I_{e6} with $[EtOx]_0/[I]_0 = 590$; (b) plot of $\ln([M]_0/[M]_t)$ vs time for the polymerizations using initiators I_3, I_{e4} and I_{e6} with $[EtOx]_0/[I]_0 = 188$; (c) linear relationship between the number of triflate initiating groups per initiator and the propagation rate constant k_p^{app} for the polymerizations using initiators I_1, I_3, I_{e4} and I_{e6} with $[EtOx]_0/[I]_0 = 188$ or I_1, I_3, I_4 and I_{e6} with $[EtOx]_0/[I]_0 = 590$ (only the linear part of the graph is included in the fits).

and 2-ethyl-2-oxazoline may arise from the nature of solvent and the used monomer concentrations. All the samples were dried and analyzed by DMF SEC. As for PMeOx, a linear increase of M_n versus conversion is observed for the polymerizations of EtOx initiated by I_3, I_4 and I_{e6} (Fig. 8). This tends to prove that polymerizations of high polymerization degree star PEtOx occur without transfer reaction. Again, all the measured M_n are lower than the expected one because of the use of PMMA standard calibration.

Using large monomer to initiator ratio often hides the initiation step. Thus a kinetic study was conducted with $[EtOx]_0/[I]_0$ ratio set to 188 and to verify the independence of k_p^{app} with respect of the $X_{n\ targeted}$. The kinetics using the three pluritriflate initiators I_3, I_{e4} and I_{e6} were investigated. Samples were periodically taken and ^{1}H NMR analyses of the reaction medium were conducted before the active centers deactivation. The pseudo-first order plot, $\ln([M]_0/[M]_t)$ vs time (Fig. 7b), is presented for the three initiators, and a linear relationship is observed after 40 min of reaction. Interestingly, the linearity is not observed at low polymerization time, which suggests a slow initiation. A linear fit of the final points was made and was represented in solid line on Fig. 7b. The k_p^{app} calculated from the slopes of the linear part are plotted against the number of initiator functions on Fig. 7c and the k_p^{app} values are similar to the values obtained with $[EtOx]_0/[I]_0 = 590$, confirming that k_p^{app} values do not depend on the $[EtOx]_0/[I]_0$ ratio (Table S1).

The ^{1}H NMR analysis of samples before any quenching allowed the highlighting of ionic propagating species, on the basis of Saegusa's [35,47] and Lapinte's [48] work. The peaks corresponding to CH_2-O (a) and CH_2-N (b) of oxazolinium end chains appear respectively at 4.64 and 4.05 ppm (Fig. 9). This assignment is confirmed by a COSY NMR experiment (Fig. S20), that also shows the coupling between protons (d) and (e) of the residual monomer. The integrations of the peaks of oxazolinium end chains at 4.64 ppm, residual monomer at 3.92 ppm and polymer at 3.14 ppm are used to calculate the oxazolinium end chains percentage. The ionic species percentage (defined as the number of measured oxazolinium end chains to the total number of end chains) was plotted as a function of conversion (Fig. 10). This percentage increases with the polymerization and reaches a constant value of around 85–90% for a conversion higher than 35%. This value is in good agreement with the kinetic plots (Fig. 7b), where linearity started at a similar time, meaning that all the propagating species are formed. In this study, we make the assumption that the incertitude of the NMR analyses might be higher than the usual 5% since the peaks of the

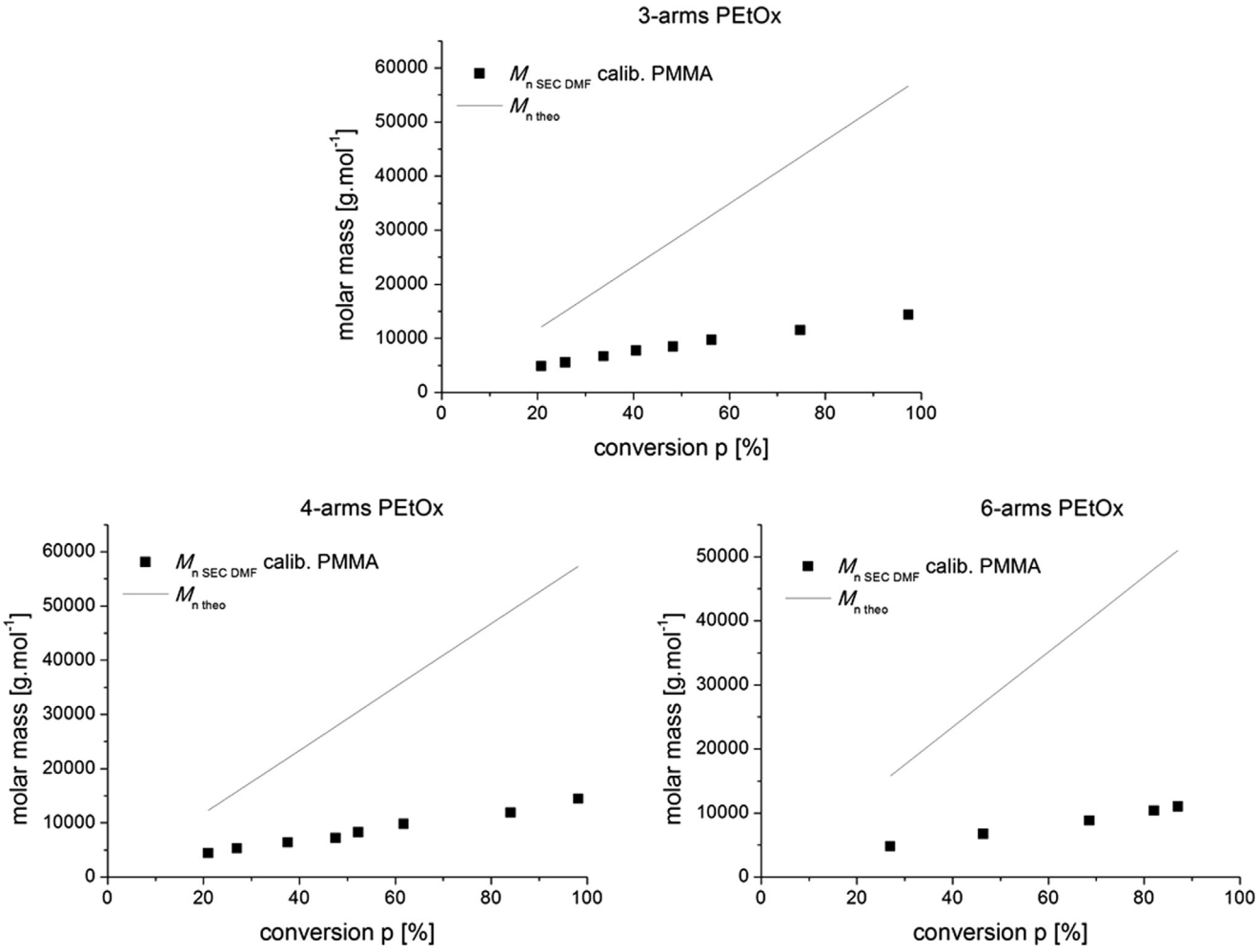

Fig. 8. Molar masses of 3-, 4-, and 6-arm stars PEtOx with $[EtOx]_0/[I]_0$ = 590 as a function of conversion.

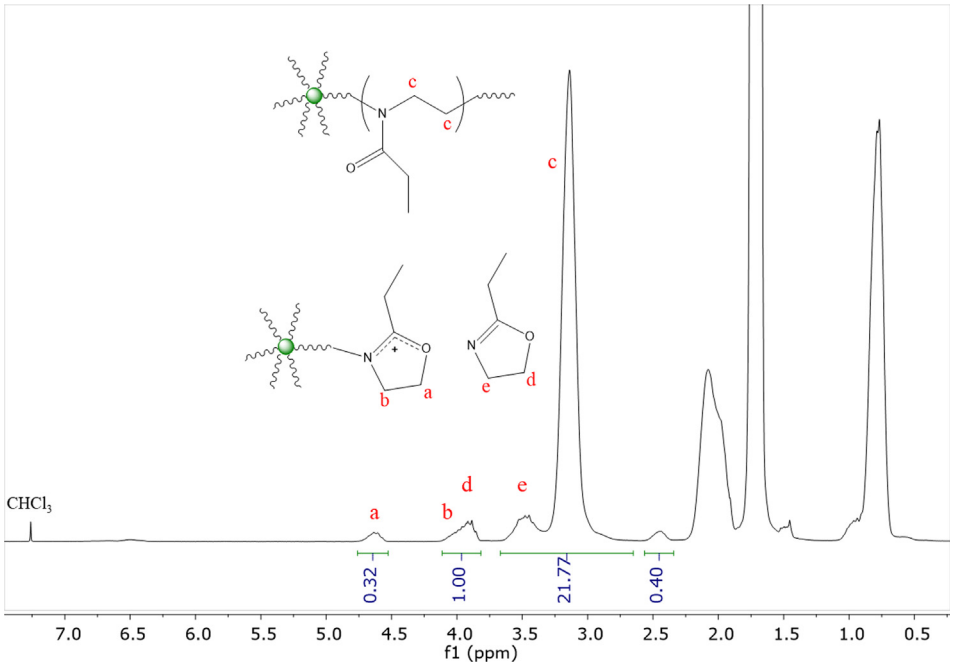

Fig. 9. ^{1}H NMR spectrum of the 8th sampling of the polymerization initiated by I_{e6} with $[EtOx]_0/[I]_0$ = 188 in $CDCl_3$.

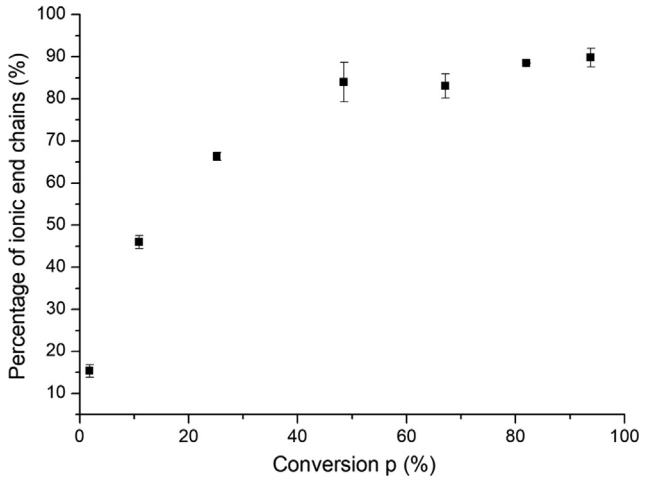

Fig. 10. Percentage of ionic end chains calculated from the ^{1}H NMR spectra of samplings versus conversion. Polymerization initiated by I_{e6} with $[EtOx]_0/[I]_0 = 188$. The error bars correspond to the standard deviation from three analyses of one Free Induction Decay (FID).

oxazolinium species integrate for much lower value than the one for the monomer or the polymer (depending on the investigated reaction time), explaining the discrepancy between the measured and expected oxazolinium percentages. When using a monofunctional triflate initiator to initiate the MeOx or EtOx polymerization, it was shown that all the propagating species are ionic [2]. However, in our work, the proximity of the charges located on the multifunctional initiators at low polymerization times makes them gradually appear until the conversion reached a minimum value.

The polymerization kinetic of MeOx conducted in similar conditions provided a fast initiation, without delay to the formation of all the growing species. A first explanation is a difference of reactivity between the two monomers with the triflate functions, however no significant difference in the k_p^{app} determination was observed between the two monomers, suggesting another explanation. The initiation step of star polymers in ionic polymerization requires the formation of a large number of ionic species in the vicinity of core of the star polymers. The thermodynamic is very unfavorable for such kind of situation. Indeed, it is possible to calculate the Bjerrum length l_B, that characterizes the strength of electrostatic interactions in the solvent.

$$l_B = \frac{e_0^2}{4\pi\varepsilon_r\varepsilon_0 k_B T}$$

with:

e_0 elementary charge, $e_0 = 1.602.\ 10^{-19} A{\cdot}s$
ε_r relative dielectric constant of the medium, $\varepsilon_{r,acetonitrile}$=37.5
ε_0 vacuum permittivity, $\varepsilon_0 = 8.8542{\cdot}10^{-12} F{\cdot}m^{-1}$
k_B Boltzmann constant, $k_B = 1.38{\cdot}10^{-23} J{\cdot}K^{-1}$
T temperature, $T = 353\ \ K$
In acetonitrile, $l_B = 1.26{\cdot}10^{-9}\ \ m$

In acetonitrile, l_B is close to 13 Å, a value much larger than the distance between two triflate functions in any of the used initiators of this study. Providing that PEtOx and PMeOx have a different solubility in ACN, *i.e.* different chain extension, the thermodynamic of the formation of a second charge in the vicinity of the first one may be affected.

The kinetic analysis reveals that the initiation step observed for the 2-ethyl-2-oxazoline polymerization may be different from the one observed for 2-methyl-2-oxazoline. An average slow initiation kinetic measured for the polymerization of 2-ethyl-2-oxazoline in the presence of I_3, I_{e4} and I_{e6} suggests that the corresponding star polymers may have heterogeneous molar masses when the targeted molar mass of the star polymer is low. The heterogeneity may be alleviated for polymerization degree of 590.

4. Conclusions

In the present work, we compared poly(2-methyl-2-oxazoline) and poly(2-ethyl-2-oxazoline) star polymer syntheses. The formation of star polymers using tri, tetra and hexa functional initiators was successfully achieved with targeted molar mass close to 16 000 g mol^{-1} for the 2-methyl-2-oxazoline polymerization, and from 16 000 to 60 000 g mol^{-1} for 2-ethyl-2-oxazoline polymerization. The star structure was first demonstrated by ^{1}H NMR analyses, thanks to the agreement between the number of oxazolinium functions measured on the ^{1}H NMR spectra, and the expected arm number from the initiator. Then a kinetic study was conducted for the two monomers, and it was shown that the k_p^{app} followed a discrete increase as a function of the number of initiating site per initiator molecule. The SEC analysis using an iterative method ended to the conclusion of a consistent number of arms with respect to the used initiator, taking in account the decrease of intrinsic viscosity as a function of arms number per macromolecule, for a constant molar mass. While steric hindrance was suspected to prevent the formation of well-defined star-polymers with POx arms for I_{e6}, we observed in the present study that selecting triflate as counter-ion could prevent this limitation. However, the initiation step for the 2-ethyl-2-oxazoline polymerization was found to be slow, a phenomenon that was not detected for the 2-methyl-2-oxazoline polymerization. The steric hindrance incrimination to explain this result is thus ruled out. As for anionic systems [49,50] we believe that electrostatic repulsion between active sites requires overcoming a thermodynamic barrier that could be observed if the number of sites per initiator is high, or if the growing polymer is highly condensed (poor polymer solubility). In the present study, the issue of electrostatic repulsion between initiating sites borne by the same initiator for 2-ethyl-2-oxazoline polymerization is prevented by a slow initiation step that allowed for the synthesis of star polymers with the expected structures. The poly(2-ethyl-2-oxazoline) star polymers may have heterogeneous arm length for low molar mass, but are more homogeneous for higher targeted molar mass.

Declaration of Competing Interest

The authors certify that there is no conflict of interest issued from the present work.

Acknowledgement

This work was supported by the Fondation pour la Recherche Médicale, France, grant number PLP20161036677 to Laetitia Plet and the Agence Nationale pour la Recherche, France (ANR-17-CE18-0015-01-VINP)

Appendix A. Supplementary material

Supplementary data to this article can be found online at https://doi.org/10.1016/j.eurpolymj.2019.109323.

References

[1] T. Saegusa, S. Kobayashi, Polymerization of cyclic imino ethers, Int. Rev. Sci. Phys. Chem. Ser. 2 (8) (1975) 153–190.
[2] K. Aoi, M. Okada, Polymerization of oxazolines, Prog. Polym. Sci. 21 (1996) 151–208.
[3] Q. Liu, M. Konas, J.S. Riffle, Investigations of 2-ethyl-2-oxazoline polymerizations in chlorobenzene, Macromolecules 26 (1993) 5572–5576, https://doi.org/10.1021/ma00073a007.
[4] A. Dworak, The role of cationic and covalent active centers in the polymerization of 2-methyl-2-oxazoline initiated with benzyl bromide, Macromol. Chem. Phys. 199 (1998) 1843–1849, https://doi.org/10.1002/(SICI)1521-3935(19980901)

199:9 < 1843::AID-MACP1843 > 3.0.CO;2-I.
[5] T. Saegusa, S. Kobayashi, A. Yamada, Kinetics and mechanism of the isomerization polymerization of 2-methyl-2-oxazoline by benzyl chloride and bromide initiators. Effect of halogen counteranions, Makromol. Chem. 177 (1976) 2271–2283, https://doi.org/10.1002/macp.1976.021770805.
[6] M. Bauer, S. Schroeder, L. Tauhardt, K. Kempe, U.S. Schubert, D. Fischer, In vitro hemocompatibility and cytotoxicity study of poly(2-methyl-2-oxazoline) for biomedical applications, J. Polym. Sci., Part A: Polym. Chem. 51 (2013) 1816–1821, https://doi.org/10.1002/pola.26564.
[7] K. Aoi, H. Suzuki, M. Okada, Architectural control of sugar-containing polymers by living polymerization: ring-opening polymerization of 2-oxazolines initiated with carbohydrate derivatives, Macromolecules 25 (1992) 7073–7075, https://doi.org/10.1021/ma00051a056.
[8] S. Zalipsky, C. Lee, Poly(Ethylene Glycol) Chemistry: Biotechnical and Biomedical Applications, Springer, US, 1992.
[9] F.M. Veronese, A. Mero, G. Pasut, Protein PEGylation, basic science and biological applications, in: F.M. Veronese (Ed.), PEGylated Protein Drugs Basic Sci. Clin. Appl., Birkhäuser Basel, Basel, 2009, pp. 11–31, , https://doi.org/10.1007/978-3-7643-8679-5_2.
[10] K. Knop, R. Hoogenboom, D. Fischer, U.S. Schubert, Poly(ethylene glycol) in drug delivery: pros and cons as well as potential alternatives, Angew. Chem. Int. Ed. 49 (2010) 6288–6308, https://doi.org/10.1002/anie.200902672.
[11] J.-S. Park, K. Kataoka, Precise control of lower critical solution temperature of thermosensitive poly(2-isopropyl-2-oxazoline) via gradient copolymerization with 2-ethyl-2-oxazoline as a hydrophilic comonomer, Macromolecules 39 (2006) 6622–6630, https://doi.org/10.1021/ma0605548.
[12] N. ten Brummelhuis, H. Schlaad, Stimuli-responsive star polymers through thiol–yne core functionalization/crosslinking of block copolymer micelles, Polym. Chem. 2 (2011) 1180, https://doi.org/10.1039/c1py00002k.
[13] G. Le Fer, C. Amiel, G. Volet, Copolymers based on azidopentyl-2-oxazoline: synthesis, characterization and LCST behavior, Eur. Polym. J. 71 (2015) 523–533, https://doi.org/10.1016/j.eurpolymj.2015.08.028.
[14] R. Hoogenboom, M.W.M. Fijten, G. Kickelbick, U.S. Schubert, Synthesis and crystal structures of multifunctional tosylates as basis for star-shaped poly(2-ethyl-2-oxazoline)s, Beilstein J. Org. Chem. 6 (2010) 773–783, https://doi.org/10.3762/bjoc.6.96.
[15] A. Dworak, R.C. Schulz, Star polymers and block copolymers of 2-oxazolines using chloroformates as initiators, Macromol. Chem. Phys. 192 (1991) 437–445.
[16] B. Rasolonjatovo, B. Pitard, T. Haudebourg, V. Bennevault, P. Guégan, Synthesis of tetraarm star block copolymer based on polytetrahydrofuran and poly(2-methyl-2-oxazoline) for gene delivery applications, Eur. Polym. J. 88 (2017) 689–700, https://doi.org/10.1016/j.eurpolymj.2016.09.042.
[17] R. Weberskirch, R. Hettich, O. Nuyken, D. Schmaljohann, B. Voit, Synthesis of new amphiphilic star polymers derived from a hyperbranched macroinitiator by the cationic 'grafting from' method, Macromol. Chem. Phys. 200 (1999) 863–873, https://doi.org/10.1002/(SICI)1521-3935(19990401)200:4 < 863::AID-MACP863 > 3.0.CO;2-N.
[18] C. Lach, R. Hanselmann, H. Frey, R. Mülhaupt, Hyperbranched carbosilane oxazoline-macromonomers: polymerization and coupling to a trimesic acid core, Macromol. Rapid Commun. 19 (1998) 461–465, https://doi.org/10.1002/(SICI)1521-3927(19980901)19:9 < 461::AID-MARC461 > 3.0.CO;2-8.
[19] C. Zhang, S. Liu, L. Tan, H. Zhu, Y. Wang, Star-shaped poly(2-methyl-2-oxazoline)-based films: rapid preparation and effects of polymer architecture on antifouling properties, J. Mater. Chem. B. 3 (2015) 5615–5628, https://doi.org/10.1039/C5TB00732A.
[20] L.Y. Qiu, Y.H. Bae, Polymer architecture and drug delivery, Pharm. Res. 23 (2006) 1–30, https://doi.org/10.1007/s11095-005-9046-2.
[21] K. Yasugi, Y. Nagasaki, M. Kato, K. Kataoka, Preparation and characterization of polymer micelles from poly(ethylene glycol)-poly(d, l-lactide) block copolymers as potential drug carrier, J. Control. Rel. 62 (1999) 89–100, https://doi.org/10.1016/S0168-3659(99)00028-0.
[22] M. Kovár, J. Strohalm, T. Etrych, K. Ulbrich, B. Říhová, Star structure of antibody-targeted HPMA copolymer-bound doxorubicin: a novel type of polymeric conjugate for targeted drug delivery with potent antitumor effect, Bioconjug. Chem. 13 (2002) 206–215.
[23] E.R. Gillies, E. Dy, J.M.J. Fréchet, F.C. Szoka, Biological evaluation of polyester dendrimer: poly(ethylene oxide) "bow-tie" hybrids with tunable molecular weight and architecture, Mol. Pharm. 2 (2005) 129–138, https://doi.org/10.1021/mp049886u.
[24] M. Bauer, C. Lautenschlaeger, K. Kempe, L. Tauhardt, U.S. Schubert, D. Fischer, Poly(2-ethyl-2-oxazoline) as alternative for the stealth polymer poly(ethylene glycol): comparison of in vitro cytotoxicity and hemocompatibility, Macromol. Biosci. 12 (2012) 986–998, https://doi.org/10.1002/mabi.201200017.
[25] R. Luxenhofer, M. Bezen, R. Jordan, Kinetic investigations on the polymerization of 2-oxazolines using pluritriflate initators, Macromol. Rapid Commun. 29 (2008) 1509–1513.
[26] T. Ogoshi, S. Hiramitsu, T. Yamagishi, Y. Nakamoto, Columnar stacks of star- and tadpole-shaped polyoxazolines having triphenylene moiety and their applications for synthesis of wire-assembled gold nanoparticles, Macromolecules 42 (2009) 3042–3047, https://doi.org/10.1021/ma900169j.
[27] D.-P. Yang, M.N.N.L. Oo, G.R. Deen, Z. Li, X.J. Loh, Nano-star-shaped polymers for drug delivery applications, Macromol. Rapid Commun. 38 (2017), https://doi.org/10.1002/marc.201700410.
[28] H.M.L. Lambermont-Thijs, M.W.M. Fijten, U.S. Schubert, R. Hoogenboom, Star-shaped poly(2-oxazoline)s by dendrimer endcapping, Aust. J. Chem. 64 (2011) 1026, https://doi.org/10.1071/CH11128.
[29] G. Pereira, C. Huin, S. Morariu, V. Bennevault-Celton, P. Guégan, Synthesis of poly(2-methyl-2-oxazoline) star polymers with a β-cyclodextrin core, Aust. J. Chem. 65 (2012) 1145–1155, https://doi.org/10.1071/CH12232.
[30] J. Jeerupan, T. Ogoshi, S. Hiramitsu, K. Umeda, T. Nemoto, G. Konishi, T. Yamagishi, Y. Nakamoto, Star-shaped poly(2-methyl-2-oxazoline) using by reactive bromoethyl group modified calix[4]resorcinarene as a macrocyclic initiator, Polym. Bull. 59 (2008) 731–737, https://doi.org/10.1007/s00289-007-0809-2.
[31] K.-M. Kim, Y. Ouchi, Y. Chujo, Synthesis of organic-inorganic star-shaped polyoxazolines using octafunctional silsesquioxane as an initiator, Polym. Bull. 49 (2003) 341–348, https://doi.org/10.1007/s00289-002-0113-0.
[32] C. Huin, Z. Eskandani, N. Badi, A. Farcas, V. Bennevault-Celton, P. Guégan, Anionic ring-opening polymerization of ethylene oxide in DMF with cyclodextrin derivatives as new initiators, Carbohydr. Polym. 94 (2013) 323–331, https://doi.org/10.1016/j.carbpol.2012.12.062.
[33] F.M. Menger, V.A. Migulin, Synthesis and properties of multiarmed geminis, J. Org. Chem. 64 (1999) 8916–8921, https://doi.org/10.1021/jo9912350.
[34] V. Bennevault-Celton, A. Urbach, O. Martin, C. Pichon, P. Guégan, P. Midoux, Supramolecular assemblies of histidinylated α-cyclodextrin in the presence of DNA scaffold during CDplexes formation, Bioconjug. Chem. 22 (2011) 2404–2414, https://doi.org/10.1021/bc200167p.
[35] T. Saegusa, H. Ikeda, H. Fujii, Isomerization polymerization of 2-oxazoline. IV. Kinetic study of 2-methyl-2-oxazoline polymerization, Macromolecules 5 (1972) 359–362, https://doi.org/10.1021/ma60028a005.
[36] B. Guillerm, S. Monge, V. Lapinte, J.-J. Robin, How to modulate the chemical structure of polyoxazolines by appropriate functionalization, Macromol. Rapid Commun. 33 (2012) 1600–1612, https://doi.org/10.1002/marc.201200266.
[37] R. Hoogenboom, M.W.M. Fijten, U.S. Schubert, Parallel kinetic investigation of 2-oxazoline polymerizations with different initiators as basis for designed copolymer synthesis, J. Polym. Sci. Part Polym. Chem. 42 (2004) 1830–1840, https://doi.org/10.1002/pola.20024.
[38] A. Kowalczuk, J. Kronek, K. Bosowska, B. Trzebicka, A. Dworak, Star poly(2-ethyl-2-oxazoline)s-synthesis and thermosensitivity, Polym. Int. 60 (2011) 1001–1009, https://doi.org/10.1002/pi.3103.
[39] M. Glassner, D.R. D'hooge, J.Y. Park, P.H.M. Van Steenberge, B.D. Monnery, M.-F. Reyniers, R. Hoogenboom, Systematic investigation of alkyl sulfonate initiators for the cationic ring-opening polymerization of 2-oxazolines revealing optimal combinations of monomers and initiators, Eur. Polym. J. 65 (2015) 298–304, https://doi.org/10.1016/j.eurpolymj.2015.01.019.
[40] B. Rasolonjatovo, J.-P. Gomez, W. Meme, C. Gonçalves, C. Huin, V. Bennevault-Celton, T. Le Gall, T. Montier, P. Lehn, H. Cheradame, P. Midoux, P. Guégan, Poly(2-methyl-2-oxazoline)-b-poly(tetrahydrofuran)-b-poly(2-methyl-2-oxazoline) amphiphilic triblock copolymers: synthesis, physicochemical characterizations, and hydrosolubilizing properties, Biomacromolecules 16 (2015) 748–756, https://doi.org/10.1021/bm5016656.
[41] B.H. Zimm, W.H. Stockmayer, The dimensions of chain molecules containing branches and rings, J. Chem. Phys. 17 (1949) 1301–1314, https://doi.org/10.1063/1.1747157.
[42] B.H. Zimm, R.W. Kilb, Dynamics of branched polymer molecules in dilute solution, J. Polym. Sci. 37 (1959) 19–42, https://doi.org/10.1002/pol.1959.1203713102.
[43] J.A. Burns, D.M. Haddleton, C.R. Becer, Synthesis and SEC Characterization of Poly(methyl methacrylate) Star Polymers, in: K. Matyjaszewski, B.S. Sumerlin, N.V. Tsarevsky (Eds.), Prog. Control. Radic. Polym. Mater. Appl., American Chemical Society, Washington, DC, 2012, pp. 81–98, , https://doi.org/10.1021/bk-2012-1101.ch006.
[44] C. Jackson, D.J. Frater, J.W. Mays, Dilute solution properties of asymmetric six-arm star polystyrenes, J. Polym. Sci. Part B Polym. Phys. 33 (1995) 2159–2166, https://doi.org/10.1002/polb.1995.090331507.
[45] S.T. Balke, T.H. Mourey, D.R. Robello, T.A. Davis, A. Kraus, K. Skonieczny, Quantitative analysis of star-branched polymers by multidetector size-exclusion chromatography, J. Appl. Polym. Sci. 85 (2002) 552–570, https://doi.org/10.1002/app.10539.
[46] R.M. Paulus, C.R. Becer, R. Hoogenboom, U.S. Schubert, Acetyl halide initiator screening for the cationic ring-opening polymerization of 2-ethyl-2-oxazoline, Macromol. Chem. Phys. 209 (2008) 794–800, https://doi.org/10.1002/macp.200700506.
[47] T. Saegusa, H. Ikeda, Isomerization polymerization of 2-oxazoline. VI. Kinetic study on the polymerization of 2-methyl-2-oxazoline initiated by methyl iodide, Macromolecules 6 (1973) 808–811, https://doi.org/10.1021/ma60036a004.
[48] B. Guillerm, S. Monge, V. Lapinte, J.-J. Robin, Novel investigations on kinetics and polymerization mechanism of oxazolines initiated by iodine, Macromolecules 43 (2010) 5964–5970, https://doi.org/10.1021/ma1009808.
[49] X.-S. Feng, D. Taton, E.L. Chaikof, Y. Gnanou, Toward an easy access to dendrimer-like poly(ethylene oxide)s, J. Am. Chem. Soc. 127 (2005) 10956–10966, https://doi.org/10.1021/ja0509432.
[50] N. Badi, L. Auvray, P. Guégan, Synthesis of half-channels by the anionic polymerization of ethylene oxide initiated by modified cyclodextrin, Adv. Mater. 21 (2009) 4054–4057, https://doi.org/10.1002/adma.200802982.